

Methods for Carbon Mass Closure in Polyolefin Hydrocracking

Anna E. Brenner, Griffin Drake, Gregg T. Beckham, and Yuriy Román-Leshkov*



Cite This: https://doi.org/10.1021/jacsau.5c00476



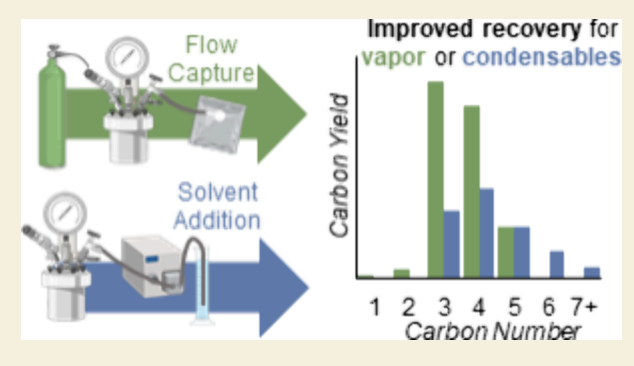
ACCESS I

Metrics & More

Article Recommendations

Supporting Information

ABSTRACT: Heterogeneous catalytic hydrocracking of polyolefins is a promising approach for the processing of postconsumer plastics, but product quantification methods remain inconsistent across the literature. In systems that generate a large fraction of vapor-phase products, typical product capture methods can result in large carbon balance deficits, exceeding 50%, compromising reported yields and selectivities. Here, we identify the major sources of product loss and develop enhanced capture methods to improve the quantification accuracy. Seven supplemental techniques were evaluated, targeting either increased vapor recovery (by increasing the volatility or system volume) or enhanced retention in the liquid phase (by decreasing volatility). Among these, a flow collection approach using a continuous



helium sweep and downstream gas sampling bag capture yielded the highest recovery, achieving a $96 \pm 9.2\%$ carbon balance closure. We show that the efficacy of these methods is strongly dependent on product distribution. In general, solvent addition was most effective when condensable species dominate the product distribution, while flow collection was preferred when both condensable species and light gases are present in high concentrations. These results highlight the need for method-specific workup strategies and demonstrate that no single protocol is universally optimal. We provide general guidelines for selecting and implementing robust product capture techniques, enabling accurate yield and selectivity determinations in polyolefin hydrocracking systems.

KEYWORDS: Plastics Deconstruction, Polyethylene, Hydrocracking, ZSM-5, Gas Chromatography, Carbon Balance

■ INTRODUCTION

Heterogeneous catalytic hydrocracking has emerged as a promising approach for the chemical deconstruction of postconsumer polyolefins, enabling the upcycling of this waste carbon resource. 1-6 The design of effective catalytic systems for this process has benefited from extensive prior research on alkane hydrocracking, which has elucidated the interplay between metallic and Brønsted acidic sites in C-C bond cleavage reactions. In polyolefin hydrocracking, hydrogen is incorporated during bond-scission events to generate saturated products of lower molecular weight (Figure 1A). When cleavage predominantly occurs at metal sites ("hydrogenolysis"), the primary products are methane and a distribution of larger linear alkanes (nC_x) , eventually converging to full methanation at sufficiently long contact times.⁸⁻³⁸ In contrast, Brønsted acid catalysts promote isomerization and β -scission ("bifunctional hydrocracking"), suppressing methane formation and favoring the production of smaller, branched iso-alkanes (iC_x) . 39-56 Catalysts with high acid-to-metal site ratios, or those lacking metal sites entirely, produce volatile hydrocarbon distributions, reflecting the dominance of β -scission cracking pathways mediated by Brønsted acid sites ("acid catalytic cracking"). However, unlike traditional acid catalytic cracking, which generates large quantities of alkenes and aromatics, the combination of monofunctional acid catalysts with high-pressure hydrogen

during polyolefin deconstruction produces predominantly saturated alkane species. As hydrogen-rich acid catalytic cracking and bifunctional hydrocracking processes for polyethylene exist on a continuum and share similar product distributions, we refer to both processes collectively here as "hydrocracking."

The products of polyolefin hydrocracking are typically classified into four physical phases under ambient temperature and pressure: (1) a vapor phase (or "headspace") containing light and volatile species, (2) a liquid phase of solubilized hydrocarbons, (3) an oligomeric "wax" phase composed of low-melting solids, and (4) a solid phase comprising unreacted polymer, potential coke deposits, and spent catalyst. The precise carbon range associated with each phase depends on both the chemical product distribution and the specific postreaction isolation method. For example, wax-phase species may be recovered as solids or remain dissolved in the liquid phase, depending on the liquid product yield, as well as the workup solvent volume and temperature. Typically, the objective of

Received: April 21, 2025 Revised: July 8, 2025 Accepted: July 9, 2025



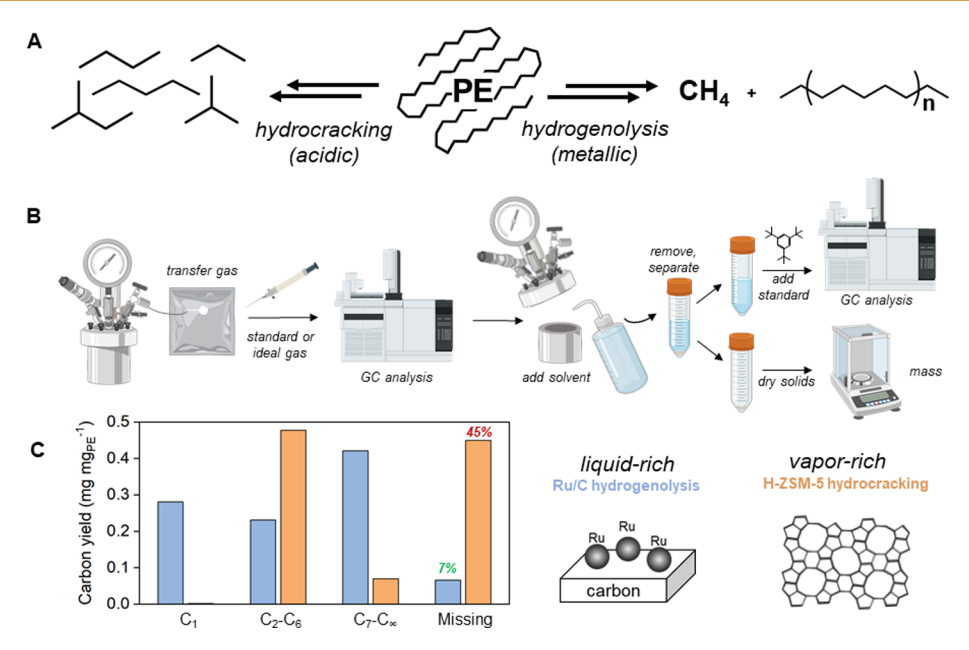


Figure 1. (A) Simplified comparison of the most abundant hydrogenolysis and hydrocracking process products. (B) Schematic diagram of a typical workup method for gaseous and liquid/solid products. (C) Representative carbon distribution for product produced through hydrocracking (orange) and hydrogenolysis ¹⁴ (blue), as achieved by the schematic workup method shown in (B). Ru/C reaction conditions: 700 mg of PE, 25 mg of 5 wt % Ru/C, 200 °C, 16 h, 20 barg of H₂ fill, 600 rpm. ¹⁴ Reproduced from ref 14. Copyright 2021 American Chemical Society. H-ZSM-5 reaction conditions: 700 mg of PE, 330 mg of H-ZSM-5, 250 °C, 4 h, 40 barg of H₂ fill, 600 rpm.

polyolefin hydrocracking is to funnel carbon from the polymer substrate into a narrow product distribution, maximizing activity while minimizing methane formation.⁴⁴

Most hydrocracking studies reported in the peer-reviewed literature are performed in batch reactors at modest product scales ($\sim 0.1-10$ g). The "workup method" for product analysis typically follows three main steps: (1) capture of material from the reactor, (2) compositional analysis, and (3) selection of a quantitation basis. Workup methods vary by phase, where vapor-phase products are usually captured in gas sampling bags, analyzed by gas chromatography (GC) with flame ionization detection (FID) or mass spectrometry detection (MS) (Figure 1B), and quantified using one of three approaches: (1) an ideal gas approximation of the total moles, based on reactor pressure and temperature after reaction, (2) calibration with an external hydrocarbon standard⁵⁷ or internal inert-gas standard,^{30,31} or (3) subtraction of the quantified liquid and solid carbon from the initial mass, attributing the remainder to the vapor phase. Liquid and solid products are normally extracted using solvents and quantified either gravimetrically or via external standards. 14,15 These protocols generally yield acceptable carbon balances in methane- or liquid-rich systems (Figure 1C). 14,15 However, in vapor-rich systems, such as those obtained using Co-containing zeolite catalysts previously reported by our group, 58,59 these standard methods often result in significant mass deficits. Because catalyst performance is commonly evaluated in terms of carbon yield (Y) and recovered-product selectivity (S_c) , incomplete carbon balances compromise the accuracy of these metrics. Without closure, mechanistic interpretation is hindered, and assessments of catalyst efficiency, scalability, and techno-economic feasibility become unreliable.6

Here, we identify and quantify the primary sources of carbon loss in vapor-rich polyolefin hydrocracking systems and develop supplemental product capture strategies to improve the mass balance closure. Of the seven techniques that were evaluated, a continuous sweep-gas flow into a gas sampling bag provided the most effective recovery, achieving carbon closure of $96 \pm 9.2\%$. We show that the efficacy of each method was strongly dependent on the underlying product distribution. For condensable-rich systems, solvent addition improved recovery, while sweep-gas collection was superior when both light gases and condensables were present. Finally, given that mass balances are essential for validating reported yields and selectivities, we recommend several practical guidelines for rigorous product quantification in polyolefin hydrocracking studies.

METHODS

All chemicals, equipment, and consumables are listed in Tables S1–S3.

Catalyst Pretreatment and Characterization

Commercial zeolite catalyst H-ZSM-5 (Si/Al = 11.5, Zeolyst CBV2314) was calcined (550 °C, 5 h, 5 °C min⁻¹ ramp rate, flowing air) and kept in sealed vials prior to use. Characterization of the catalyst indicates it contained roughly 10 wt % water content at time of use with a total acid site count (by ammonia temperature-programmed desorption) of 1330 μ mol g⁻¹ (Note S1, Figure S1).

Reactivity Studies

In a typical reaction, a Parr reactor (25 mL, 316 SS, Note S2, Figure S2) was charged with 700 mg of polyethylene (PE, $\sim\!4000$ Da $M_{\rm w}$, Sigma-Aldrich), 330 mg of H-ZSM-5 catalyst, and a PTFE stir bar, then sealed, flushed three times between 20 and 5 barg with H $_2$ (Linde, 99.999% UHP), and pressurized to 40 barg. The reaction is run in the absence of any solvent. Reaction time (t = 0 h) began at the initiation of heating and magnetic stirring (600 rpm), taking $\sim\!40$ min to reach the 250 °C set point, pressurizing to a final value of $\sim\!70$ barg. The reactor was heated in a machined aluminum block wrapped

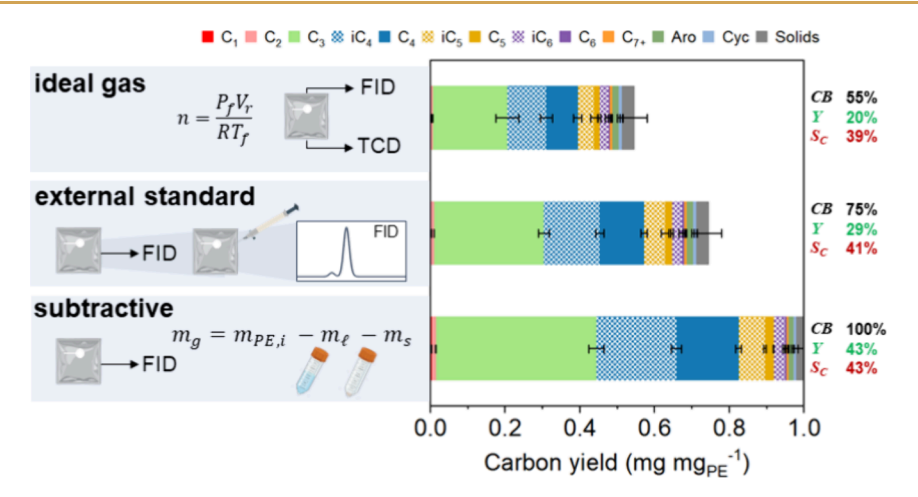


Figure 2. Product distributions and propane benchmarks for the catalytic base-case reaction using different vapor mass bases. Solid and liquid products (included) used the same workup for each mass basis. The average solids conversion was 97%. Labels are carbon balance (CB), propane carbon mass yield (Y), and recovered-product propane carbon mass selectivity (S_C). Error bars represent the standard deviation of triplicate measurements. Reaction conditions: 700 mg of PE, 330 mg of H-ZSM-5, 250 °C, 4 h, 40 barg of H₂ fill, 600 rpm. All data shown graphically here are provided in Excel S1.

with heating elements to maintain an even external temperature distribution (Figure S2). The reactor temperature was PID controlled by an internal thermocouple whose tip was 1.5" below the head. At steady-state operation, this internal temperature was within 5 °C of the temperature measured at the base of the heating block, as recommended by other investigators. At the end of the desired reaction time, the reactor was quenched in ice, reducing the temperature to below reactive levels (150 °C) within ~5 min. After further cooling, the reactor was removed from ice and equilibrated to room temperature (~20 °C) for at least 40 min for product removal and analysis. Reaction pressure conditions are reported as the fill pressure (40 barg fill) rather than the pressure observed during reaction.

Product Capture

Initial headspace products were generally captured through a short transfer line into 1, 2, or 3 L gas sampling bags (Supel-Inert, Multi-Layer Foil). A separate 0.6 L gas sampling bag was filled with pure propylene (≥99%, Sigma-Aldrich) from which 1−10 mL was injected by gastight syringe into sampling bags as an external standard; headspace products were analyzed before and after propylene addition. Remaining products were solubilized in solvent, massed, then centrifuged (11,000 rpm, 10 min). The supernatant (~30 mL) was drawn off, mixed with ~ 20 mg 1,3,5-tritertbutyl benzene (>98%, TCI) as an external standard, and diluted further (~15 vol %) for analysis. Alternative capture procedures are discussed in detail in the Results section.

Product Quantification and Calibration

Gaseous products were analyzed by manual injection of \sim 0.4 mL via gastight syringe to an Agilent 7890 gas chromatograph (GC) using flame ionization (FID) and mass spectrometry (MS) detectors using a DB-1 column. Headspace injections pre- and post-propylene addition were used to determine the relative and absolute abundance of hydrocarbon species, respectively. Hydrogen content was determined by an Agilent 8890 GC instrument with a thermal conductivity detector (TCD) using a HayeSep Q column. Solvated liquid products were analyzed by two GC systems: an Agilent 7890 GC-FID using an HP-5 column for C_{8+} species and an Agilent 7890

GC-FID using a DB-1 column for C_3 – C_6 species. Separation methods and typical chromatograms are listed in Note S3 (Figures S3-S8). Residual solids were dried and massed, determining a polymer content by subtraction of catalyst loading and/or thermogravimetric analysis. Details of calibration and sample calculations are available in the Supporting Information (SI Notes S3–S6: Figures S3-S15, Table S4, and eqs S1-S21). Uncertainties are reported in the text as ranges from duplicate experiments or standard deviations from triplicate experiments.

RESULTS

Evaluation of Typical Workup Methods for Product Analysis

We first evaluated whether the standard workup protocol, which performs well for liquid-rich systems, is suitable for vapor-rich product distributions. As a base case, we selected a previously reported zeolite-based hydrocracking system known to yield low carbon balances. 58,59 Batch reactions were performed using 700 mg of low molecular weight polyethylene (PE, ~4000 Da) in a 25 mL Parr reactor with commercial H-ZSM-5 (Zeolyst, Si/Al = 11.5) as the catalyst. Reaction conditions of 250 $^{\circ}$ C, 70 barg H₂, and a 4 h reaction time were chosen to align with prior literature reports, noting that the initial fill pressure was 40 barg H_2 . The headspace was captured in a 2 L gas sampling bag by direct transfer and analyzed by GC-FID and GC-TCD (thermal conductivity detection) both before and after the addition of propylene $(C_{3=})$ as an external standard. Details on GC calibration and sample calculations are provided in the Supporting Information (Notes S3-S6: Figures S3-S15, Table S4, and eqs S1-S21). Propylene was selected as the standard because it is not a reaction product, although any hydrocarbon may be used if introduced after a baseline injection (Figure S12, eq S6). Liquid-phase products were extracted with *n*-heptane, quantified using 1,3,5-tri-tert-butylbenzene (TTBB) as an external standard, and waxes were estimated gravimetrically following solvent evaporation. The remaining catalyst/polymer residue was dried and weighed to determine solid-phase carbon.

To assess the robustness of the method, we applied identical liquid/solid workups and vapor analyses to the base-case system but varied the quantitation basis for vapor-phase products. Three distinct interpretations of the same reaction were generated using (1) the ideal gas mole count, (2) an external standard calibration, or (3) subtraction of liquid and solid carbon from the initial mass. The resulting product distributions are shown in Figure 2. Qualitatively, the vaporphase fraction was dominated by propane (C₃), isobutane (iC_4) , and *n*-butane (nC_4) , with minor amounts of higher *n*alkanes and iso-alkanes, and negligible methane (Figure S3). Trace alkenes were detected at shorter reaction times (Figure S16). These distributions are consistent with acid-catalyzed hydrocracking mechanisms reported for zeolites. 40,43-45,50,53,56 In the absence of metal sites, zeolite acid sites catalyze dehydrogenation, β -scission, and hydrogenation sequences, 61,62 terminating at C₃ and C₄ products due to limited further β -scission. Residual solids were minimal, with the average conversion reaching 97%, and no soluble waxes were detected, confirming near-complete conversion and a vaporrich, iso-alkane-dominated product distribution. Such high conversion is common in literature reports, where systems are often optimized to maximize the product yield. Despite similar selectivities across quantitation methods, the ideal gas basis yielded only 55 \pm 6.4% carbon recovery and the external standard basis 75 \pm 9.6%, while the subtractive method substantially overestimated propane yield. These discrepancies motivated further analysis of the underlying assumptions on each vapor quantitation basis.

The ideal gas method assumes vapor-phase ideality and complete capture upon expansion. To test this assumption, we partitioned the reactor headspace (final pressure of ~40 barg) into four sequential 1 L gas sampling bags, each lowering the pressure by ~10 barg. If ideal, then the product distribution should be constant across samples. However, we observed that early samples withdrawn at high reactor pressures were enriched in propane, while later samples taken at lower pressures were enriched in heavier products (Figure S17). This suggests an initial vapor-liquid equilibrium that is disturbed during sampling, leading to preferential evaporation of lighter species. Consequentially, partial condensation of product alkanes would underestimate the vapor molar quantity under the ideal gas law, contributing to a low carbon balance. Moreover, partial gas sampling, especially with volume-limited setups (e.g., 1 L sampling bags for 500 mL reactors), can bias the composition toward more volatile species. Accurately capturing the vapor-phase requires total depressurization and accounting for phase partitioning to avoid the systematic underestimation of heavier, condensable alkanes.

The external standard method assumes sufficient vapor capture to provide a complete carbon balance, as the standard is added only to the collected product and does not account for vapor remaining in the reactor. In an ideal, well-mixed 25 mL reactor at \sim 40 barg, the vapor should expand to \sim 1 L upon depressurization, meaning that a single sampling bag should recover \sim 97% of total hydrocarbons, leaving \sim 3% unquantified in the reactor. To validate this, we conducted sequential gas "rinses" after the initial sampling by refilling the sealed reactor with hydrogen and then withdrawing the new vapor into fresh sampling bags, quantifying each by external standard addition (Figure S18). These post-sampling rinses recovered significant quantities of propane and butanes (in excess of the expected \sim 3%) (Figure S19), indicating either

incomplete initial extraction and/or the presence of condensed C_3/C_4 species. Additionally, later rinses were enriched with C_5/C_6 species (Figure S18), likely from volatilization. Consistent with the mechanism and prior reports, ⁵⁰ we hypothesized that these light alkanes, condensed at post-reaction conditions but volatile at ambient temperature, likely represent a major source of unaccounted carbon during standard workup. These findings confirm that the postreaction headspace is not ideal and cannot be efficiently captured in a single sample.

The subtractive workup method compounds these errors. More specifically, partial headspace removal biases the measured composition due to preferential distillation, while capture inefficiencies misattribute mass to the most readily recoverable species. Further, the subtractive approach provides no independent method for verifying the carbon balance in vapor-rich systems. While the external standard basis offers a calibrated vapor-phase measurement, it still underestimates total mass due to incomplete extraction. Thus, while we recommend the external standard approach over ideal gas or subtractive methods, even if this strategy fails to close the carbon balance in vapor-rich systems. We therefore sought to develop improved protocols to capture missing volatile species and ensure accurate quantitation.

Development of Improved Capture Methods

We hypothesized that the missing fraction consists of C₅/C₆ species, which are expected hydrocracking products, that remain in the liquid phase during headspace workup but escape when the reactor is unsealed. Note that at 20 $^{\circ}\text{C}$ in a sealed 25 mL reactor, 100 mg of pure iso-pentane partitions 56% into the vapor phase, compared to only 1.6% for *n*-octane. Alternatively, complete volatilization of 100 mg of iso-pentane requires expansion to a system volume of just 44 mL, while noctane requires 1520 mL (Note S7, eqs S22-S25). To test this hypothesis, we evaluated seven supplemental capture methods designed to either force these species into the vapor phase (by increasing the volatility or system volume) or retain them in the liquid phase (by decreasing the volatility). The effectiveness of each extraction method for the base-case condition is summarized in Figure 3, along with estimated total vapor capture and analysis times, which generally exceeded those of conventional liquid workup. Consideration of the workup time is important for maintaining sufficient throughput, particularly if a method requires specialized equipment (e.g., flow controllers or chromatography instruments) that may be difficult to parallelize. All reactions were performed to the same degree of near-complete solid conversion (96%) to avoid any convoluting effects from the extent of reaction. The typical method—external standard-based vapor capture with propylene and liquid-phase extraction using TTBB—served as the baseline, yielding ~75% carbon recovery. Most supplemental capture methods improved the overall carbon balance by 10–15% and were enriched in C_5/C_6 species, supporting the hypothesis that these species are lost during typical workups. However, the extent of recovery and the associated time varied across methods, with some approaches providing more complete product capture, as discussed below.

The "extra gas rinses" method, used previously to probe capture efficiency, provided incremental gains with diminishing returns, as each additional rinse extracted progressively less hydrocarbon (Figure S18). Repressurizing the reactor between rinses (20 barg fill) likely re-established vapor—liquid

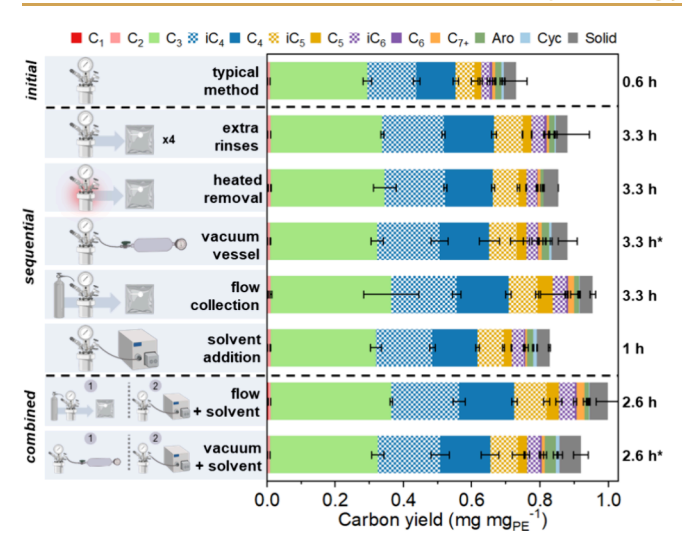


Figure 3. Comparison of capture methods for targeting intermediate products. The average solid conversion was 96%. Typical method uses a single 2 L sampling bag for direct capture and manual liquid workup. Sequential methods are applied following direct headspace capture. Combined methods capture all vapor products together and then apply solvent addition. Error bars represent the range of duplicate measurements and standard deviation of triplicate measurements (only for the typical method). Times to the right of the plot correspond to total workup and chromatographic analysis time for the given approaches. *Additional time (\sim 5 h) was allowed for the "vacuum extraction" method to achieve a well-mixed system after standard addition. Reaction conditions: 700 mg PE, 330 mg H-ZSM-5, 250 °C, 4 h, 40 barg H₂ fill, 600 rpm. All data shown graphically here are provided in Excel S1.

equilibrium, limiting the volatilization of residual products. Lower-pressure rinses also impeded capture, as a larger fraction of vapor remained in the reactor during sampling. Although each rinse was fast, the total analysis time increased substantially due to the generation of five separate vapor samples, raising consumable costs and processing overhead (or requiring additional sampling bag evacuation prep time).

The "heated removal" method involved pre-equilibrating the reactor at 60 °C and 20 barg of N_2 under agitation (600 rpm) for 2 h, followed by direct transfer of the headspace to a gas sampling bag. A temperature of 60 °C was chosen as it is within the safe operating limits of the gas bag (80 °C) but significantly increases the vapor pressure of C_5/C_6 products (estimated ~3.5x for *iso*-pentane). While more effective than a single room-temperature gas rinse, this method failed to recover significant additional carbon, likely because the temperature increase was insufficient to overcome system pressure, limiting its ability to shift the vapor—liquid equilibrium. Moreover, the extended equilibration time reduced throughput, and further heating risked recondensation during ambient sampling. Temperature limitations of gas sampling bags further constrain the utility of this method.

The "vacuum extraction" method aimed to promote volatilization by reducing the system pressure. Drawing from approaches in hydrogen-free reactions, 57 we employed a 2.25 L vacuum-tight vessel (Figure S20), sized to contain the full pressurized headspace while remaining below atmospheric pressure to facilitate future combined trials (*vide infra*). The vessel was pre-evacuated to <0.1 mbar, then connected to the reactor via a 1/4" steel transfer line, allowing the vapor to expand under the established static vacuum (\sim 25 in. Hg) for 2

h. After capture, the propylene standard was injected and allowed to equilibrate for ~5 h before sampling. We found empirically that equilibration for ~1 h could lead to a biased propane/propylene ratio (Figure S21) and, therefore adopted 5 h as a safe protocol. The lack of complete hydrocarbon recovery as vapor, which is the expected equilibrium condition, was not achieved. A similar test using a 1/8" transfer line recovered minimal product, suggesting a vapor transport limitation may be relevant. While moderately effective, this method appears inherently diffusion-limited under low-pressure gradients.

The "flow collection" method (Figure S22) proved the most effective, achieving full carbon closure (96 ± 9.2%). This approach enhances product recovery by continuously flowing helium through the reactor (10 mL min⁻¹), increasing the total gas volume, and reducing hydrocarbon partial pressures to promote volatilization. Unlike static extractions, flow collection steadily strips the reactor of residual vapor-phase species, preventing recondensation and product loss during depressurization. This distinguishes it from vacuum extraction, which is constrained by vapor transport, and from gas rinses, which require repressurization that reinstates vapor-liquid equilibrium. A key advantage of flow collection is its ability to capture the integral composition of all extracted vapors rather than instantaneous snapshots of headspace composition. In contrast, inline GC sampling during depressurization or purging measures the transient vapor-phase distribution at discrete time points, potentially misrepresenting the overall product composition in highly dynamic systems (Figures S17– S18). Although flow collection is highly effective, it is limited by the need for large gas volumes.

Given the difficulty of volatilizing intermediate species, we next tested the "solvent addition" method, hypothesizing that liquid-phase nonidealities contribute to carbon loss for vaporonly recovery. Specifically, this method leverages solvent effects to retain volatile hydrocarbons in solution and prevent their loss upon unsealing the reactor. n-Heptane was chosen for this study to avoid any overlap with C₅/C₆ species in GC quantification while remaining sufficiently low-boiling for ease of solids drying. Other solvents used in the hydrogenolysis literature, including acetone or dichloromethane, were shown to have a direct overlap in retention time with C_5/C_6 species (Figure S7). Solvent selection should be tailored to each product distribution to minimize interference and maximize product quantification. To test this, we introduced *n*-heptane into the sealed reactor, maintaining low hydrocarbon partial pressures and suppressing volatilization during extraction. Solvent introduction risks pressurization, which can eject material. To mitigate this, n-heptane was delivered using an HPLC pump at 1 mL min⁻¹ over 20 min rather than injecting solvent manually via a syringe, as in prior work.⁵⁷ While less effective for total recovery—likely due to poor retention of C₃/ C₄ alkanes—solvent addition solubilized many compounds otherwise captured in the vapor phase (Figure 3, Figure S23). This establishes solvent addition as a complementary method to vapor-phase capture, as it provides rapid stabilization and prevents the immediate loss of intermediates upon reactor unsealing. However, its performance depends on solventhydrocarbon interactions, with n-heptane offering limited retention of lighter species. Optimization with solvents of higher polarity, boiling point, or hydrogen-bonding capacity, as well as temperature control, may further improve recovery.

To integrate the strengths of individual methods, we tested combined protocols that paired vapor-phase recovery with solvent-based stabilization. In the "combined flow collection", the initial reactor headspace was first captured into a 3 L gas sampling bag. Without disconnecting the transfer line, helium was then flowed continuously through the reactor (10 mL min⁻¹) into the same bag. Following gas collection, 20 mL of solvent was added to the sealed reactor. This approach combined the two stages of headspace capture (initial + flow collection) with a final solvent rinse. The "combined flow collection" method performed comparably to sequential flow collection but offered greater reliability, likely due to reduced sampling losses during changeover between gas sampling bags. The "combined vacuum extraction" was performed using the same vacuum vessel described previously but omitted initial headspace removal. Instead, the postreaction headspace (~40 barg) was directly vented into the vessel and allowed to expand under a static vacuum of ~5 in. Hg for 2 h. The reduced vacuum strength relative to the "vacuum extraction" method results from the greater quantity of gas introduced into the fixed-volume capture vessel. Following gas expansion, 20 mL of solvent was added to the sealed reactor. In contrast to the improved recovery from the "combined flow collection," the "combined vacuum extraction" yielded no increased recovery relative to its noncombined counterpart, but resulted in a higher fraction of solubilized products (Figure S23). This outcome can be attributed to the weaker vacuum in the combined case compared to the sequential vacuum extraction, limiting its capacity to generate a strong driving force for vapor-phase extraction. To probe the effect of extraction further, we repeated the "vacuum extraction" using a vessel backfilled with nitrogen to ~10 in. Hg. The resulting intermediate degree of vapor capture (versus capture in solvent) confirmed the importance of vacuum strength on the extraction (Figure S24). The addition of solvent at the final stage helped to retain volatile hydrocarbons that would otherwise escape upon depressurization. In this setup, solvent addition was complementary when combined with flow collection, as it retained only intermediates not captured by the sweep gas flow, but compensatory when combined with vacuum capture, as it solubilized unextracted volatiles. This highlights the inherent ambiguity in defining "liquid yield," which is strongly influenced by workup methodology in polyolefin hydrocracking.

With a complete carbon balance, the true product selectivity from Figure 3 can be compared to the best estimate of the external standard method (Figure 2). While C_4 selectivity remained unchanged at 36%, the true C_3 selectivity is lower (37 \pm 2.5% versus 40 \pm 3.3%) and the true C_5/C_6 selectivity is higher (18 \pm 0.3% versus 14 \pm 1.4%). Additionally, this closure provides confirmation of the lack of soluble waxes or other major product classes. The improved accuracy also enabled quantitative assessments of C–C bond scission sitetime yields (\sim 0.009 mol C–C g_{cat}^{-1} h⁻¹, eq S20) and net hydrogen consumption (\sim 29%, eq S21), calculations that would otherwise require assumptions about missing species.

While combined methods offered the most complete recovery, their utility depends on experimental constraints such as reactor geometry, vapor-phase transport efficiency, and equipment throughput. Among all techniques evaluated, flow collection remains the most effective approach for capturing volatile species, although as mentioned previously, it requires significant gas volumes. Specifically, there is a minimum

quantity of gas required to volatilize a given product by reducing its partial pressure below its vapor pressure (Note S7). This impacts scalability; larger product masses require more sweep gas to volatilize. A slow flow of gas in perfect equilibrium would in theory achieve maximum utilization, but in practice, faster (and less volume-efficient) flow is likely needed for sufficient throughput. With that noted, there are opportunities for further optimization to improve utilization. Additional agitation or heat may be applied during collection to hasten equilibration so long as the total gas volume remains sufficient. If the collection of large individual sample volumes is difficult, multiple small samples may be drawn in reusable sampling bags, which has the advantage of allowing timeresolved observation of when effective removal is ceased. If cost is limiting, helium may be replaced with another sweep gas not detected by GC-FID. Ultimately, carbon balance permitting, adjustments to a method adopted in a specific laboratory setting are recommended.

Region of Method Applicability

Standard product workup methods typically yield acceptable carbon balances in liquid-rich hydrocracking systems. Significant mass deficits arise only when volatile intermediates accumulate, necessitating more rigorous product capture. To define the conditions under which extended capture procedures become essential, we evaluated carbon closure as a function of reaction time using a simplified workup protocol consisting of direct headspace sampling, followed by a single gas rinse (Figure S25). Between 1 and 4 h, the carbon balance remained constant at ~65%, even as solid conversion increased from \sim 65% to \sim 95%. At longer reaction times (8–40 h) and complete solid conversion, the carbon balance gradually improved, eventually reaching closure as C_1-C_4 hydrocarbons accumulated. This time series suggests that the reaction proceeds in two stages: a rapid conversion of solid polymer into light intermediates, many of which are lost in conventional workups (2-4 h), followed by a slower transformation of these intermediates into readily capturable vapor-phase products (20 h). The slower conversion of intermediates to terminal products is likely driven by volatility constraints in liquidphase contacting, resulting in an unintentional reactive separation.^{36,63} Consequentially, solid conversion is no longer an effective proxy for reactivity in the region dominated by secondary cracking (5-20 h). The ability to capture vaporphase species was not affected by catalyst loading (Figure S26), suggesting that decreased C-C bond scission activity at extended reaction times are not due to catalyst deactivation, and difficulty of vapor capture is not attributable to strong adsorption in the zeolite. Additionally, reducing the total substrate and catalyst mass (to decrease the final product partial pressure) led to higher carbon balances (Figure S27), although these results may be convoluted by variations in reaction extent. These findings indicate that carbon balance closure is highly sensitive to reaction conditions and should be independently evaluated for each experiment.

To assess the general utility of our most effective protocol, we applied the combined flow collection method across a broad range of reaction times (1–20 h) (Figure 4) to control the concentration of volatile intermediates. As expected, at 20 h, when the majority of products had converted to light vaporphase species, the carbon balance became less sensitive to the workup method. However, at the 4 h base-case, a significant concentration of volatile intermediates remained, rendering the

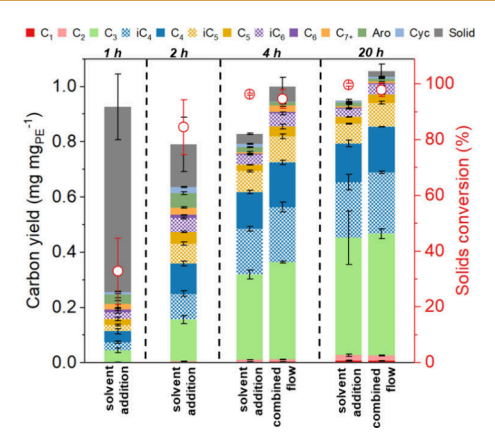


Figure 4. Product distribution for variable reaction time conditions as a function of the capture method. Error bars represent the range of duplicate (1, 4, 20 h) or triplicate (2 h) measurements. Reaction conditions: 700 mg of PE, 330 mg of H-ZSM-5, 250 $^{\circ}$ C, 40 barg of H₂ fill, 600 rpm. All data shown graphically here are provided in Excel S1.

carbon balance highly dependent on capture strategy. At 2 h, even extensive method optimization (Figure S28) failed to consistently achieve >80% carbon recovery, indicating persistent losses from transient, condensable species. Solvent addition provided a slight improvement over flow collection at this condition, though solid conversion (a proxy for reaction extent) was highly variable, further complicating interpretation. One possible explanation is that liquid-like intermediates, abundant at this condition, volatilize during flow collection but later condense in the gas sampling bag, escaping quantification. Further reducing the reaction time to 1 h improved carbon closure, likely due to a lower absolute concentration of intermediates.

These results reinforce that no single capture method is universally optimal. As the reaction proceeds and the product distribution evolves, capture strategies must be tailored accordingly. In general, we recommend solvent addition when condensable intermediates $(C_5/C_6 \text{ species})$ dominate the apparent product distribution (>30 wt % of volatile products), flow collection for moderate concentrations of intermediates (15-30 wt %), and any direct-capture method where intermediates are scarce (<15 wt %). These thresholds are empirical and contingent on the specific conditions employed; for example, increasing the hydrocarbon loading within a fixed reactor volume or decreasing the workup temperature may suppress volatilization and elevate the impact of condensable species. Critically, mass balances must be quantitatively assessed as part of all exploratory studies to validate product selectivities and guide method selection. Workup procedures should be iteratively refined to ensure closure under varying conditions and product states.

CONCLUSIONS AND GUIDELINES

We developed and experimentally validated quantification methods that achieve near-complete carbon closure for polyolefin hydrocracking, even under conditions dominated by volatile intermediates. These methods significantly improve the accuracy of yield and selectivity measurements, which are otherwise compromised by mass deficits in vapor-rich systems. The need to perform these extended capture methods depends on the chemical system. In methane-rich hydrogenolysis systems, the ideal gas law provides a reasonable vapor-phase estimate, as readily volatilized species remain low, are less

isomerized, and are often solubilized by liquid products. In contrast, Brønsted acid-catalyzed hydrocracking, particularly in the absence of metal functionality, produces transient, highly volatile intermediates that are prone to loss during conventional workup.

Although this study focused on polyethylene and H-ZSM-5, the quantification challenges that we identify are broadly applicable to other polyolefin substrates and acid-catalyzed systems. The volatility and instability of hydrocracking intermediates are intrinsic to the reaction mechanism and not specific to the catalyst identity or substrate structure. Importantly, the concentration of these intermediates (and thus the severity of mass balance errors) depends on the extent of reaction, which, in turn, will be influenced by process variables such as temperature, hydrogen pressure, and reactor scale. This variability makes it difficult to anticipate quantification issues *a priori*, reinforcing the need for empirical validation of carbon balances in each system.

Based on our findings, we recommend the following guidelines for vapor-phase product quantification in polyolefin hydrocracking:

- (1) Capture the entire headspace for analysis whenever possible. Incomplete sampling introduces systematic bias via preferential evaporation of light species. Use an external standard for calibration to ensure reliable quantitation.
- (2) Avoid subtraction-based methods for mass balance closure. These methods misattribute mass from missing species to those that are readily captured, leading to artificially inflated selectivities. If subtraction must be used, it should be benchmarked against a condition with confirmed carbon closure—but even then, product distribution sensitivity limits its reliability.
- (3) Use combined solvent addition and flow collection for maximum recovery. These methods target different volatility regimes and, when applied together, provide the most complete coverage of vapor- and liquid-phase products. Their implementation should be tailored to the product distribution.
- (4) Recognize and respond to altered carbon balances resulting from operational changes. Use the framework of volatile intermediates as primary drivers of carbon losses to guide systematic method adjustments. For example, increasing the scale of products may require a higher sweep gas volume for vaporization, reconfiguring reactor outlet fittings may necessitate longer vacuum extraction time, or improving catalyst activity may create an intermediate-rich distribution requiring solvent addition. Make carbon closure an ongoing, dynamic effort in experimentation.

While no single workup method is universally optimal, these guidelines provide a framework for designing reliable (and high-throughput) workup protocols under varying reaction conditions. As the field moves toward more advanced hydrocracking processes, ensuring that product capture methods remain accurate, quantitative, and operationally feasible will be critical for mechanistic studies, catalyst benchmarking, and techno-economic analysis.

ASSOCIATED CONTENT

Supporting Information

The Supporting Information is available free of charge at https://pubs.acs.org/doi/10.1021/jacsau.5c00476.

Chemicals, equipment, and consumables used; experimental procedures and setup; catalyst characterization; gas chromatography methods; gas chromatograph calibration procedures; sample calculations for carbon balance; re-expression of manuscript data by compound class or phase of capture; variation in carbon balance as a function of process parameters; effect of additional workup procedures on low reaction time experiments (PDF)

Additional data (XLSX)

AUTHOR INFORMATION

Corresponding Author

Yuriy Román-Leshkov — Department of Chemical Engineering, Massachusetts Institute of Technology, Cambridge, Massachusetts 02139, United States; orcid.org/0000-0002-0025-4233; Email: yroman@mit.edu

Authors

Anna E. Brenner – Department of Chemical Engineering, Massachusetts Institute of Technology, Cambridge, Massachusetts 02139, United States; orcid.org/0000-0003-3669-2515

Griffin Drake – Department of Chemical Engineering, Massachusetts Institute of Technology, Cambridge, Massachusetts 02139, United States

Gregg T. Beckham — Renewable Resources and Enabling Sciences Center, National Renewable Energy Laboratory, Golden, Colorado 80401, United States; BOTTLE Consortium, Golden, Colorado 80401, United States; orcid.org/0000-0002-3480-212X

Complete contact information is available at: https://pubs.acs.org/10.1021/jacsau.5c00476

Author Contributions

A.E.B. and G.D. contributed equally to this work.

Notes

The authors declare no competing financial interest.

ACKNOWLEDGMENTS

Funding was provided by the U.S. Department of Energy, Office of Energy Efficiency and Renewable Energy, Advanced Materials and Manufacturing Technologies Office (AMMTO) and Bioenergy Technologies Office (BETO). This work was performed as part of the Bio-Optimized Technologies to keep Thermoplastics out of Landfills and the Environment (BOTTLE) Consortium and was supported by AMMTO and BETO under Contract No. DE-AC36-08GO28308 with the National Renewable Energy Laboratory (NREL). The BOTTLE Consortium includes members from MIT, funded under Contract DE-AC36-08GO28308 with NREL. The views expressed in the article do not necessarily represent the views of the DOE or the U.S. Government. Supplemental graphics were provided by BioRender. The authors thank Joel Miscall at NREL for assistance with high-temperature gel permeation

chromatography and thermogravimetric analysis. The authors would also like to thank Marcos Garcia Farpón, Eva Andrés Marcos, Jamison Watson, Matthew Webber, Julie Rorrer, and Guido Zichitella for helpful discussions and assistance with experiments and gas chromatography methods.

REFERENCES

- (1) Kots, P. A.; Vance, B. C.; Vlachos, D. G. Polyolefin plastic waste hydroconversion to fuels, lubricants, and waxes: A comparative study. *Reaction Chemistry & Engineering* **2021**, *7* (1), 41–54.
- (2) Chu, M. Y.; Liu, Y.; Lou, X. X.; Zhang, Q.; Chen, J. X. Rational design of chemical catalysis for plastic recycling. *ACS Catal.* **2022**, *12* (8), 4659–4679.
- (3) Dong, Z. W.; Chen, W. J.; Xu, K. Q.; Liu, Y.; Wu, J.; Zhang, F. Understanding the structure-activity relationships in catalytic conversion of polyolefin plastics by zeolite-based catalysts: A critical review. ACS Catal. 2022, 12 (24), 14882–14901.
- (4) Hinton, Z. R.; Talley, M. R.; Kots, P. A.; Le, A. V.; Zhang, T.; Mackay, M. E.; Kunjapur, A. M.; Bai, P.; Vlachos, D. G.; Watson, M. P.; Berg, M. C.; Epps, T. H.; Korley, L. T. J. Innovations toward the valorization of plastics waste. *Annu. Rev. Mater. Res.* **2022**, *52*, 249–280
- (5) Wei, J. D.; Liu, J. Y.; Zeng, W. H.; Dong, Z. C.; Song, J. K.; Liu, S. B.; Liu, G. Z. Catalytic hydroconversion processes for upcycling plastic waste to fuels and chemicals. *Catalysis Science & Technology* **2023**, *13* (5), 1258–1280.
- (6) Sun, J. K.; Dong, J. H.; Gao, L. J.; Zhao, Y. Q.; Moon, H.; Scott, S. L. Catalytic upcycling of polyolefins. *Chem. Rev.* **2024**, *124*, 9457.
- (7) Weitkamp, J. Catalytic hydrocracking: Mechanisms and versatility of the process. *ChemCatChem.* **2012**, *4* (3), 292–306.
- (8) Celik, G.; Kennedy, R. M.; Hackler, R. A.; Ferrandon, M.; Tennakoon, A.; Patnaik, S.; LaPointe, A. M.; Ammal, S. C.; Heyden, A.; Perras, F. A.; Pruski, M.; Scott, S. L.; Poeppelmeier, K. R.; Sadow, A. D.; Delferro, M. Upcycling single-use polyethylene into high-quality liquid products. *ACS Central Science* **2019**, *5* (11), 1795–1803.
- (9) Tennakoon, A.; Wu, X.; Paterson, A. L.; Patnaik, S.; Pei, Y. C.; LaPointe, A. M.; Ammal, S. C.; Hackler, R. A.; Heyden, A.; Slowing, I. I.; Coates, G. W.; Delferro, M.; Peters, B.; Huang, W. Y.; Sadow, A. D.; Perras, F. A. Catalytic upcycling of high-density polyethylene via a processive mechanism. *Nature Catalysis* **2020**, *3* (11), 893–901.
- (10) Jaydev, S. D.; Martín, A. J.; Pérez-Ramírez, J. Direct conversion of polypropylene into liquid hydrocarbons on carbon-supported platinum catalysts. *ChemSusChem* **2021**, *14* (23), 5179–5185.
- (11) Jia, C. H.; Xie, S. Q.; Zhang, W. L.; Intan, N. N.; Sampath, J.; Pfaendtner, J.; Lin, H. F. Deconstruction of high-density polyethylene into liquid hydrocarbon fuels and lubricants by hydrogenolysis over Ru catalyst. *Chem. Catalysis* **2021**, *1* (2), 437–455.
- (12) Kots, P. A.; Liu, S. B.; Vance, B. C.; Wang, C.; Sheehan, J. D.; Vlachos, D. G. Polypropylene plastic waste conversion to lubricants over Ru/TiO2 catalysts. *ACS Catal.* **2021**, *11* (13), 8104–8115.
- (13) Nakaji, Y.; Tamura, M.; Miyaoka, S.; Kumagai, S.; Tanji, M.; Nakagawa, Y.; Yoshioka, T.; Tomishige, K. Low-temperature catalytic upgrading of waste polyolefinic plastics into liquid fuels and waxes. *Appl. Catal., B* **2021**, *285*, 119805.
- (14) Rorrer, J. E.; Beckham, G. T.; Roman-Leshkov, Y. Conversion of polyolefin waste to liquid alkanes with Ru-based catalysts under mild conditions. *JACS Au* **2021**, *I* (1), 8–12.
- (15) Rorrer, J. E.; Troyano-Valls, C.; Beckham, G. T.; Roman-Leshkov, Y. Hydrogenolysis of polypropylene and mixed polyolefin plastic waste over Ru/C to produce liquid alkanes. *ACS Sustainable Chem. Eng.* **2021**, *9* (35), 11661–11666.
- (16) Chen, L.; Meyer, L. C.; Kovarik, L.; Meira, D.; Pereira-Hernandez, X. I.; Shi, H.; Khivantsev, K.; Gutiérrez, O. Y.; Szanyi, J. Disordered, sub-nanometer Ru structures on CeO2 are highly efficient and selective catalysts in polymer upcycling by hydrogenolysis. ACS Catal. 2022, 12 (8), 4618–4627.
- (17) Chen, L. X.; Zhu, Y. F.; Meyer, L. C.; Hale, L. V.; Le, T. T.; Karkamkar, A.; Lercher, J. A.; Gutierrez, O. Y.; Szanyi, J. Effect of

- reaction conditions on the hydrogenolysis of polypropylene and polyethylene into gas and liquid alkanes. *Reaction Chemistry & Engineering* **2022**, *7* (4), 844–854.
- (18) Kots, P. A.; Xie, T.; Vance, B. C.; Quinn, C. M.; de Mello, M. D.; Boscoboinik, J. A.; Wang, C.; Kumar, P.; Stach, E. A.; Marinkovic, N. S.; Ma, L.; Ehrlich, S. N.; Vlachos, D. G. Electronic modulation of metal-support interactions improves polypropylene hydrogenolysis over ruthenium catalysts. *Nat. Commun.* **2022**, *13* (1), 5186.
- (19) Tamura, M.; Miyaoka, S.; Nakaji, Y.; Tanji, M.; Kumagai, S.; Nakagawa, Y.; Yoshioka, T.; Tomishige, K. Structure-activity relationship in hydrogenolysis of polyolefins over Ru/support catalysts. *Applied Catalysis B: Environmental* **2022**, 318, 121870.
- (20) Wu, X.; Tennakoon, A.; Yappert, R.; Esveld, M.; Ferrandon, M. S.; Hackler, R. A.; LaPointe, A. M.; Heyden, A.; Delferro, M.; Peters, B.; Sadow, A. D.; Huang, W. Y. Size-controlled nanoparticles embedded in a mesoporous architecture leading to efficient and selective hydrogenolysis of polyolefins. *J. Am. Chem. Soc.* **2022**, *144* (12), 5323–5334.
- (21) Borkar, S. S.; Helmer, R.; Panicker, S.; Shetty, M. Investigation into the reaction pathways and catalyst deactivation for polyethylene hydrogenolysis over silica-supported cobalt catalysts. *ACS Sustainable Chem. Eng.* **2023**, *11* (27), 10142–10157.
- (22) Chauhan, M.; Antil, N.; Rana, B.; Akhtar, N.; Thadhani, C.; Begum, W.; Manna, K. Isoreticular metal-organic frameworks confined mononuclear Ru-hydrides enable highly efficient shape-selective hydrogenolysis of polyolefins. *JACS Au* **2023**, 3 (12), 3473–3484.
- (23) Chen, S. J.; Tennakoon, A.; You, K. E.; Paterson, A. L.; Yappert, R.; Alayoglu, S.; Fang, L. Z.; Wu, X.; Zhao, T. Y.; Lapak, M. P.; Saravanan, M.; Hackler, R. A.; Wang, Y. Y.; Qi, L.; Delferro, M.; Li, T.; Lee, B. Y. D.; Peters, B.; Poeppelmeier, K. R.; Ammal, S. C.; Bowers, C. R.; Perras, F. A.; Heyden, A.; Sadow, A. D.; Huang, W. Y. Ultrasmall amorphous zirconia nanoparticles catalyse polyolefin hydrogenolysis. *Nature Catalysis* **2023**, *6*, 161.
- (24) Chu, M.; Wang, X.; Wang, X.; Lou, X.; Zhang, C.; Cao, M.; Wang, L.; Li, Y.; Liu, S.; Sham, T.-K.; Zhang, Q.; Chen, J. Site-selective polyolefin hydrogenolysis on atomic Ru for methanation suppression and liquid fuel production. *Research* **2023**, *6*, 0032.
- (25) Jaydev, S. D.; Usteri, M.-E.; Martín, A. J.; Pérez-Ramírez, J. Identifying selective catalysts in polypropylene hydrogenolysis by decoupling scission pathways. *Chem. Catalysis* **2023**, 3 (5), 100564.
- (26) Ji, H.; Wang, X.; Wei, X.; Peng, Y.; Zhang, S.; Song, S.; Zhang, H. Boosting polyethylene hydrogenolysis performance of Ru-CeO2 catalysts by finely regulating the Ru sizes. *Small* **2023**, *19* (35), 2300903.
- (27) Kang, Q.; Chu, M.; Xu, P.; Wang, X.; Wang, S.; Cao, M.; Ivasenko, O.; Sham, T.-K.; Zhang, Q.; Sun, Q.; Chen, J. Entropy confinement promotes hydrogenolysis activity for polyethylene upcycling. *Angew. Chem., Int. Ed.* **2023**, *62* (47), No. e202313174.
- (28) Lee, S.; Shen, K.; Wang, C.-Y.; Vohs, J. M.; Gorte, R. J. Hydrogenolysis of n-eicosane over Ru-based catalysts in a continuous flow reactor. *Chemical Engineering Journal* **2023**, *456*, 141030.
- (29) Lu, S.; Jing, Y.; Jia, S.; Shakouri, M.; Hu, Y.; Liu, X.; Guo, Y.; Wang, Y. Enhanced production of liquid alkanes from waste polyethylene via the electronic effect-favored Csecondary-Csecondary bond cleavage. *ChemCatChem.* **2023**, *15* (3), No. e202201375.
- (30) Meirow, M.; Tennakoon, A.; Wu, X.; Willmon, J.; Howell, D.; Huang, W.; Sadow, A. D.; Luijten, E. Influence of pore length on hydrogenolysis of polyethylene within a mesoporous support architecture. J. Phys. Chem. C 2023, 127 (49), 23805–23813.
- (31) Tennakoon, A.; Wu, X.; Meirow, M.; Howell, D.; Willmon, J.; Yu, J.; Lamb, J. V.; Delferro, M.; Luijten, E.; Huang, W.; Sadow, A. D. Two mesoporous domains are better than one for catalytic deconstruction of polyolefins. *J. Am. Chem. Soc.* **2023**, *145* (32), 17936–17944.
- (32) Vance, B. C.; Kots, P. A.; Wang, C.; Granite, J. E.; Vlachos, D. G. Ni/SiO2 catalysts for polyolefin deconstruction via the divergent hydrogenolysis mechanism. *Appl. Catal., B* **2023**, 322, 122138.

- (33) Chu, M.; Wang, X.; Wang, X.; Xu, P.; Zhang, L.; Li, S.; Feng, K.; Zhong, J.; Wang, L.; Li, Y.; He, L.; Cao, M.; Zhang, Q.; Chi, L.; Chen, J. Layered double hydroxide derivatives for polyolefin upcycling. *J. Am. Chem. Soc.* **2024**, *146* (15), 10655–10665.
- (34) Hu, P.; Zhang, C.; Chu, M.; Wang, X.; Wang, L.; Li, Y.; Yan, T.; Zhang, L.; Ding, Z.; Cao, M.; Xu, P.; Li, Y.; Cui, Y.; Zhang, Q.; Chen, J.; Chi, L. Stable interfacial ruthenium species for highly efficient polyolefin upcycling. *J. Am. Chem. Soc.* **2024**, *146* (10), 7076–7087.
- (35) Jaydev, S. D.; Martín, A. J.; Garcia, D.; Chikri, K.; Pérez-Ramírez, J. Assessment of transport phenomena in catalyst effectiveness for chemical polyolefin recycling. *Nature Chemical Engineering* **2024**, *1*, 565.
- (36) Wang, Y. Y.; Tennakoon, A.; Wu, X.; Sahasrabudhe, C.; Qi, L.; Peters, B. G.; Sadow, A. D.; Huang, W. Y. Catalytic hydrogenolysis of polyethylene under reactive separation. *ACS Catal.* **2024**, *14* (3), 2084–2094.
- (37) Wu, X.; Wang, X.; Zhang, L.; Wang, X.; Song, S.; Zhang, H. Polyethylene upgrading to liquid fuels boosted by atomic Ce promoters. *Angew. Chem., Int. Ed.* **2024**, *63* (8), No. e202317594.
- (38) Yuan, Y.; Xie, Z.; Turaczy, K. K.; Hwang, S.; Zhou, J.; Chen, J. G. Controlling product distribution of polyethylene hydrogenolysis using bimetallic RuM3 (M = Fe, Co, Ni) catalysts. *Chem. & Bio Engineering* **2024**, *1* (1), 67–75.
- (39) Bin Jumah, A.; Anbumuthu, V.; Tedstone, A. A.; Garforth, A. A. Catalyzing the hydrocracking of low density polyethylene. *Ind. Eng. Chem. Res.* **2019**, *58* (45), 20601–20609.
- (40) Liu, S. B.; Kots, P. A.; Vance, B. C.; Danielson, A.; Vlachos, D. G. Plastic waste to fuels by hydrocracking at mild conditions. *Science Advances* **2021**, *7* (17), eabf8283.
- (41) Vance, B. C.; Kots, P. A.; Wang, C.; Hinton, Z. R.; Quinn, C. M.; Epps, T. H.; Korley, L. T. J.; Vlachos, D. G. Single pot catalyst strategy to branched products via adhesive isomerization and hydrocracking of polyethylene over platinum tungstated zirconia. *Appl. Catal., B* **2021**, *299*, 120483.
- (42) Wang, C.; Xie, T. J.; Kots, P. A.; Vance, B. C.; Yu, K. W.; Kumar, P.; Fu, J. Y.; Liu, S. B.; Tsilomelekis, G.; Stach, E. A.; Zheng, W. Q.; Vlachos, D. G. Polyethylene hydrogenolysis at mild conditions over ruthenium on tungstated zirconia. *JACS Au* **2021**, *1* (9), 1422–1434
- (43) Lee, W. T.; van Muyden, A.; Bobbink, F. D.; Mensi, M. D.; Carullo, J. R.; Dyson, P. J. Mechanistic classification and benchmarking of polyolefin depolymerization over silica-lumina-based catalysts. *Nat. Commun.* 2022, 13 (1), 4850.
- (44) Rorrer, J. E.; Ebrahim, A. M.; Questell-Santiago, Y.; Zhu, J.; Troyano-Valls, C.; Asundi, A. S.; Brenner, A. E.; Bare, S. R.; Tassone, C. J.; Beckham, G. T.; Roman-Leshkov, Y. Role of bifunctional Ru/acid catalysts in the selective hydrocracking of polyethylene and polypropylene waste to liquid hydrocarbons. *ACS Catal.* **2022**, *12* (22), 13969–13979.
- (45) Chen, L.; Moreira, J. B.; Meyer, L. C.; Szanyi, J. Efficient and selective dual-pathway polyolefin hydro-conversion over unexpectedly bifunctional M/TiO2-anatase catalysts. *Applied Catalysis B: Environmental* **2023**, 335, 122897.
- (46) Du, B.; Chen, X.; Ling, Y.; Niu, T.; Guan, W.; Meng, J.; Hu, H.; Tsang, C.-W.; Liang, C. Hydrogenolysis-isomerization of waste polyolefin plastics to multibranched liquid alkanes. *ChemSusChem* **2023**, *16* (3), No. e202202035.
- (47) Kots, P. A.; Doika, P. A.; Vance, B. C.; Najmi, S.; Vlachos, D. G. Tuning high-density polyethylene hydrocracking through mordenite zeolite crystal engineering. *ACS Sustainable Chem. Eng.* **2023**, *11* (24), 9000–9009.
- (48) Li, L.; Luo, H.; Shao, Z.; Zhou, H.; Lu, J.; Chen, J.; Huang, C.; Zhang, S.; Liu, X.; Xia, L.; Li, J.; Wang, H.; Sun, Y. Converting plastic wastes to naphtha for closing the plastic loop. *J. Am. Chem. Soc.* **2023**, 145 (3), 1847–1854.
- (49) Qiu, Z.; Lin, S.; Chen, Z.; Chen, A.; Zhou, Y.; Cao, X.; Wang, Y.; Lin, B.-L. A reusable, impurity-tolerant and noble metal-free

- catalyst for hydrocracking of waste polyolefins. Science Advances 2023, 9 (25), No. eadg5332.
- (50) Tan, J. Z.; Hullfish, C. W.; Zheng, Y.; Koel, B. E.; Sarazen, M. L. Conversion of polyethylene waste to short chain hydrocarbons under mild temperature and hydrogen pressure with metal-free and metal-loaded MFI zeolites. *Applied Catalysis B: Environmental* **2023**, 338, 123028.
- (51) Wang, H.; Yoskamtorn, T.; Zheng, J.; Ho, P.-L.; Ng, B.; Tsang, S. C. E. Ce-promoted ptsn-based catalyst for hydrocracking of polyolefin plastic waste into high yield of gasoline-range products. *ACS Catal.* **2023**, *13* (24), 15886–15898.
- (52) Han, X.; Zhou, X.; Ji, T.; Zeng, F.; Deng, W.; Tang, Z.; Chen, R. Boosting the catalytic performance of metal-zeolite catalysts in the hydrocracking of polyolefin wastes by optimizing the nanoscale proximity. *EES Catalysis* **2024**, *2* (1), 300–310.
- (53) Lamb, J. V.; Lee, Y.-H.; Sun, J.; Byron, C.; Uppuluri, R.; Kennedy, R. M.; Meng, C.; Behera, R. K.; Wang, Y.-Y.; Qi, L.; Sadow, A. D.; Huang, W.; Ferrandon, M. S.; Scott, S. L.; Poeppelmeier, K. R.; Abu-Omar, M. M.; Delferro, M. Supported platinum nanoparticles catalyzed carbon-carbon bond cleavage of polyolefins: Role of the oxide support acidity. ACS Appl. Mater. Interfaces 2024, 16 (9), 11361–11376.
- (54) Shang, J.; Li, Y.; Hu, Y.; Zhang, T.; Wang, T.; Zhang, J.; Yan, H.; Liu, Y.; Chen, X.; Feng, X.; Zhang, X.; Yang, C.; Chen, D. Engineering non-noble Ni/WOx-ZrO2 towards boosted fuels production by catalytic upcycling of polyethylene at mild conditions. *J. Catal.* 2024, 430, 115302.
- (55) Tan, J. Z.; Ortega, M.; Miller, S. A.; Hullfish, C. W.; Kim, H.; Kim, S.; Hu, W.; Hu, J. Z.; Lercher, J. A.; Koel, B. E.; Sarazen, M. L. Catalytic consequences of hierarchical pore architectures within MFI and FAU zeolites for polyethylene conversion. *ACS Catal.* **2024**, *14* (10), 7536–7552.
- (56) Vance, B. C.; Yuliu, Z.; Najmi, S.; Selvam, E.; Granite, J. E.; Yu, K.; Ierapetritou, M. G.; Vlachos, D. G. Unlocking naphtha from polyolefins using Ni-based hydrocracking catalysts. *Chemical Engineering Journal* **2024**, 487, 150468.
- (57) Lee, Y. H.; Sun, J. K.; Scott, S. L.; Abu-Omar, M. M. Quantitative analyses of products and rates in polyethylene depolymerization and upcycling. *Star Protocols* **2023**, *4* (4), 102575.
- (58) Zichittella, G.; Ebrahim, A. M.; Zhu, J.; Brenner, A. E.; Drake, G.; Beckham, G. T.; Bare, S. R.; Rorrer, J. E.; Roman-Leshkov, Y. Hydrogenolysis of polyethylene and polypropylene into propane over cobalt-based catalysts. *JACS Au* **2022**, *2* (10), 2259–2268.
- (59) Zichittella, G.; Ebrahim, A. M.; Zhu, J.; Brenner, A. E.; Drake, G.; Beckham, G. T.; Bare, S. R.; Rorrer, J. E.; Román-Leshkov, Y. Retraction of "hydrogenolysis of polyethylene and polypropylene into propane over cobalt-based catalysts". *JACS Au* **2024**, *4* (2), 865–865.
- (60) Nicholson, S. R.; Rorrer, J. E.; Singh, A.; Konev, M. O.; Rorrer, N. A.; Carpenter, A. C.; Jacobsen, A. J.; Roman-Leshkov, Y.; Beckham, G. T. The critical role of process analysis in chemical recycling and upcycling of waste plastics. *Annu. Rev. Chem. Biomol. Eng.* 2022, 13, 301–324.
- (61) Gounder, R.; Iglesia, E. Catalytic hydrogenation of alkenes on acidic zeolites: Mechanistic connections to monomolecular alkane dehydrogenation reactions. *J. Catal.* **2011**, 277 (1), 36–45.
- (62) Arora, S. S.; Bhan, A. Kinetics of aromatics hydrogenation on HBEA. *J. Catal.* **2020**, 383, 24–32.
- (63) Kim, C. A.; Sahasrabudhe, C. A.; Wang, Y.-Y.; Yappert, R.; Heyden, A.; Huang, W.; Sadow, A. D.; Peters, B. Population balance equations for reactive separation in polymer upcycling. *Langmuir* **2024**, *40* (8), 4096–4107.
- (64) Beckham, G. T. Methods for carbon mass closure in polyolefin hydrocracking. Created in BioRender, 2025. https://BioRender.com/jnymj4r.